Using Aorta-Lesion-Attenuation Difference on Preoperative Contrast-enhanced Computed Tomography Scan to Differentiate Between Malignant and Benign Renal Tumors

Joseph R. Grajo, Russell S. Terry, Justin Ruoss, Blake J. Noennig, Jonathan G. Pavlinec, Shahab Bozorgmehri, Paul L. Crispen, and Li-Ming Su

OBJECTIVE To evaluate the ability of Aorta-Lesion-Attenuation Difference (ALAD) to differentiate malignant renal tumors from renal oncocytomas.

METHODS A retrospective review of preoperative computed tomography (CT) scans and surgical pathology was performed on patients undergoing partial nephrectomy for small, solid renal masses. ALAD was calculated by measuring the difference in Hounsfield units (HU) between the aorta and the lesion of interest on the same image slice on preoperative CT scan. The discriminative ability of ALAD to differentiate malignant pathology from oncocytoma was evaluated by sensitivity, specificity, positive predictive value (PPV), negative predictive value (NPV), and area under curve (AUC) using receiver operating characteristic analysis.

RESULTS A total of 227 preoperative CT scans and corresponding pathology reports were reviewed. ALAD values were calculated during the excretory and nephrographic phases. Nephrographic ALAD was able to differentiate malignant pathology from oncocytoma using a HU threshold of 24 with a sensitivity of 84%, specificity of 86%, PPV of 98%, and NPV of 33%. The AUC for malignant pathology vs oncocytoma was 0.86 (95% confidence intervals 0.77-0.96). Nephrographic ALAD was able to differentiate chromophobe renal cell carcinoma (RCC) from oncocytoma using a HU threshold of 24 with a sensitivity of 100%, specificity of 86%, PPV of 75%, and NPV of 100%. The AUC for chromophobe RCC vs oncocytoma was 0.98 (95% confidence intervals 0.91-1.00).

CONCLUSION ALAD discriminates well between chromophobe RCC and oncocytoma, which may aid in the management of patients with indeterminate diagnoses of oncocytic neoplasm on diagnostic needle biopsy. Further validation of ALAD will be necessary prior to routine use in clinical practice. UROLOGY 125: 123–130, 2019. © 2018 Elsevier Inc.

Renal neoplasms represent a heterogeneous disease of variable histologic subtypes, grades, genetics, and biologic potential.[1,2] Widespread use of cross-sectional imaging has led to an increase in the incidental detection of solid enhancing renal masses.[3] It is well established that 20%-30% of small renal masses (SRM, <4 cm) are benign, and less than a quarter of malignant tumors are thought to harbor aggressive features.[4] Of benign lesions discovered on surgical pathology, 70% are attributable to oncocytomas, which are unable to be reliably differentiated from renal cell carcinoma (RCC) on preoperative imaging.[5] Even histopathologic diagnosis of oncocytoma following core needle biopsy remains challenging.[6] This presents a clinical conundrum, as surgical overtreatment remains a significant concern and opportunity exists for exploring means to better align treatment options with each patient's unique tumor biology.

Current treatment options for clinical T1 renal masses include radical nephrectomy, nephron-sparing partial nephrectomy, or thermal ablation. Having a comprehensive understanding of each tumor's biology in the pretreatment setting is especially pertinent to elderly patients with competing morbidities and limited life expectancy who may be optimally managed with active surveillance or

Financial Disclosure: The authors declare that they have no relevant financial interests.

From the Departments of Radiology, University of Florida College of Medicine, Gainesville, FL; the Urology, University of Florida College of Medicine, Gainesville, FL; and the Epidemiology, University of Florida College of Medicine, Gainesville, FL

Address correspondence to: Joseph R. Grajo, M.D., Department of Radiology, University of Florida College of Medicine, 1600 SW Archer Road Box 100374, Gainesville, FL 32610-0374. E-mail: grajjr@radiology.ufl.edu

Submitted: October 9, 2018, accepted (with revisions): November 30, 2018

expectant management.[7,8] Given the indolent nature of a majority of SRMs, active surveillance may now be offered to all patients as initial management for tumors 2 cm or less.[9] For these reasons, there is need to reliably differentiate oncocytomas from malignant renal tumors. One such method is the Aorta-Lesion-Attenuation Difference (ALAD) determined on computed tomography (CT) imaging. ALAD was first described by Dhyani et al who demonstrated the potential to differentiate oncocytomas from chromophobe RCCs (chRCC) by comparing the relative enhancement of the index renal lesion to that of the aorta on CT scan imaging.[10] The concept of ALAD is based on attempts to noninvasively discriminate renal tumors by differences in dynamic enhancement patterns, which has been investigated by many groups in several fashions. The literature has established that oncocytoma and clear cell RCC (ccRCC) are hypervascular in the arterial phase while chRCC and papillary RCC are hypovascular.[11] Furthermore, oncocytomas typically demonstrate peak enhancement in the nephrographic phase whereas ccRCCs peak in the arterial phase.[12,13] Because oncocytomas peak in the nephrographic phase, their enhancement at this time more closely mirrors attenuation of the blood pool in the aorta compared to malignant oncocytic and ccRCCs, which demonstrate lower attenuation values relative to the aorta. The relative similarity in enhancement patterns of oncocytomas and ccRCCs (as opposed to chRCC and papillary RCCs) may be highlighted by lesser diagnostic performance of ALAD in differentiating these entities. In the current report, we evaluate the ability of ALAD to differentiate between oncocytomas and chRCC, papillary, and ccRCC in a series of patients undergoing partial nephrectomy.

METHODS

This retrospective study was approved by our Institutional Review Board and compliant with the Health Insurance Portability and Accountability Act. Requirement for informed consent was waived. The records of patients undergoing robotic assisted partial nephrectomy between May 2008 and September 2014 by a single surgeon at a single academic tertiary care center were reviewed. Preoperative CT scans performed closest to the date of surgery either at our institution or from outside institutions and surgical pathology reports from this cohort were independently reviewed.

Image Analysis

Preoperative CT scans were reviewed by a fellowship trained abdominal radiologist (JRG) who was blinded to the pathology results. Only contrast-enhanced CTs with imaging of the kidneys in the nephrographic and/or excretory phase were included for image analysis based on results from Dhyani et al demonstrating highest diagnostic performance of ALAD on these phases of contrast.[10] The nephrographic phase was defined as homogeneous enhancement of the renal cortex and medulla without excretion into the collecting system. The excretory phase was defined as excretion into the collecting system with differential enhancement of the renal cortex and medulla. CT scans of the kidneys with only the corticomedullary phase were excluded.

Region of Interest Placement

A region of interest was placed for each CT scan meeting inclusion criteria in the abdominal aorta and the renal lesion on the same axial image slice to calculate an ALAD as defined in previous work by Dhyani et al.[10] To optimizing reproducibility, the largest possible region of interest was drawn within both the aorta and the lesion of interest within the same image slice while avoiding measurement of calcifications in an atherosclerotic aorta and necrosis, scars, hemorrhage, and calcification within a heterogeneous renal mass (Fig. 1, Panels A and B).

Inter-rater Reliability

To evaluate the reproducibility of ALAD values generated by our fellowship trained abdominal radiologist, we had a radiology resident generate ALAD values on 10 selected cases in the nephrographic phase.

Statistical Analysis

Demographics and clinical characteristics were examined using one-way analysis of variance and Kruskal-Wallis tests for normally and non-normally distributed continuous variables, respectively, and chi-square or Fisher's exact tests for categorical variables. Inter-rater reliability was determined with the Kendall's coefficient of concordance and the intraclass correlation coefficient. We assessed the discriminative ability of ALAD in the nephrographic and excretory phases to differentiate various subtypes of RCC from oncocytoma and angiomyolipoma using receiver operating characteristic (ROC) curves. We reported area under curve (AUC) along with their 95% confidence intervals (CI). The optimal cut-off values were determined using Youden's J statistic.[14] We additionally calculated sensitivity, specificity, positive predictive value (PPV), and negative predictive value (NPV) for each cut-off value. All significant tests were two-sided, with a P value <.05 considered statistically significant. Statistical analyses were performed using Statistical Analysis Software version 9.4 (SAS Institute Inc., Cary, NC).

RESULTS

A total of 227 preoperative CT scans and corresponding pathology reports were reviewed. Patient demographics and tumor characteristics are presented in Table 1. Pathology review revealed 22 oncocytomas (10%), 9 angiomyolipomas (AML) (4%), 11 chRCC (5%), 37 papillary RCC (16%), and 148 ccRCC (65%). The majority of the tumors were stage T1a, 80%.

Of patients with an available preoperative CT scan, ALAD could be determined in the excretory phase in 69% (157/227) of patients and in 37% (85/227) of patients in the nephrographic phase. The optimal threshold for ALAD values to differentiate tumor histology varied between phase of CT scan (excretory and nephrographic) and tumor histology, Table 2. Inter-rater reliability on assigning ALAD values was noted to be robust between our radiology attending and resident, data presented in Supplemental Table 1.

Mean ALAD values in the excretory phase were 37 ± 31 for AML, 27 ± 14 for chRCC, 23 ± 19 for ccRCC, 13 ± 9 for oncocytoma, and 32 ± 11 for papillary RCC (P = .002, Fig. 2, panel A). The sensitivity, specificity, PPV, and NPV of ALAD in the excretory phase to differentiate tumor histology is demonstrated in Table 2. The ability of ALAD in the excretory phase to discriminate between renal tumor

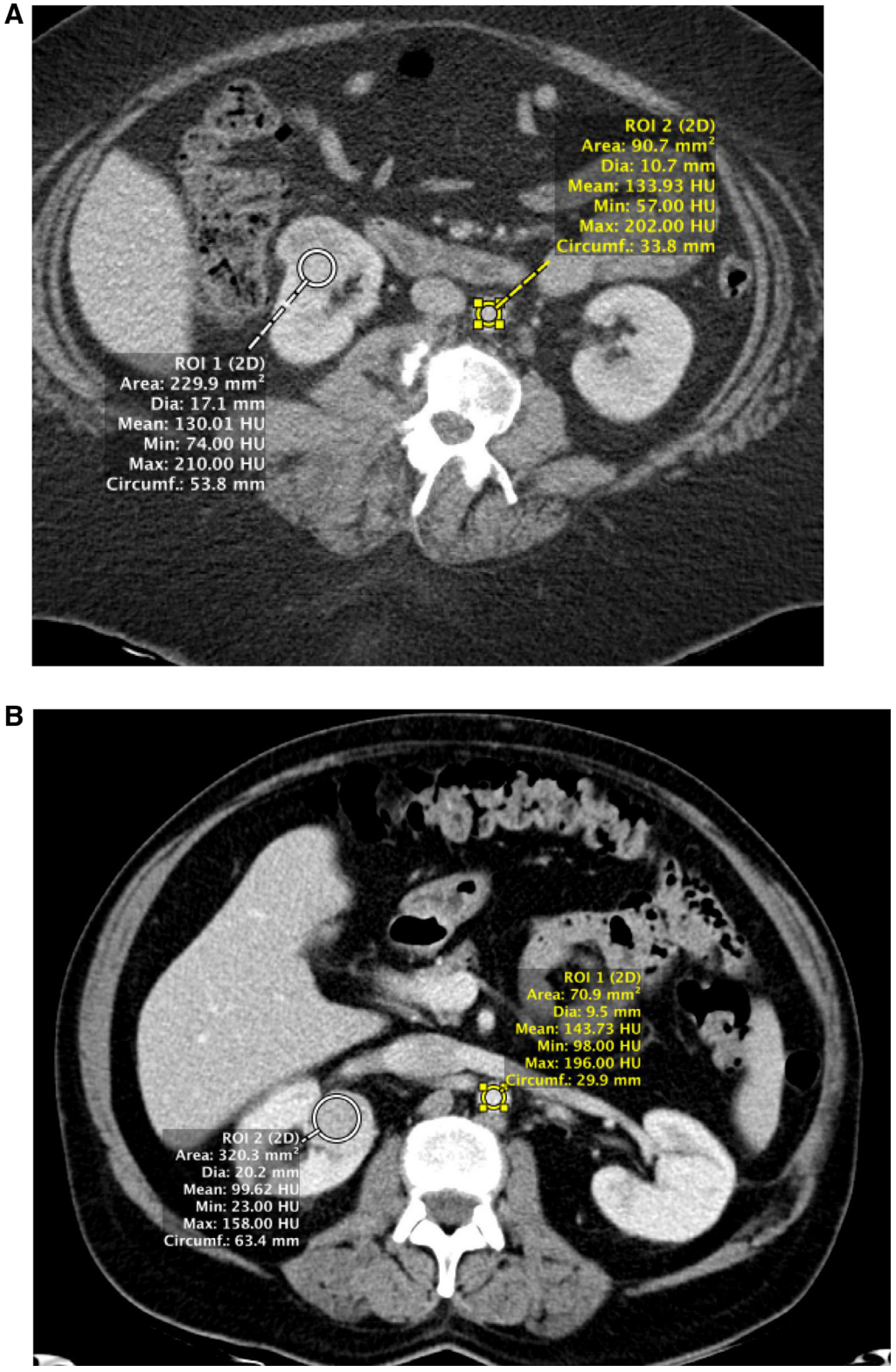

Figure 1. **Panel A:** Contrast-enhanced CT scan of a 39-year-old female with a right renal mass in the nephrographic phase (note: homogeneous enhancement of the renal cortex and medulla). The largest possible region of interest was placed in the abdominal aorta and renal lesion on the same axial slice. The low-attenuation scar in the renal mass was avoided in the region of interest placement. These measurements yielded an Aorta-Lesion-Attenuation Difference of 4 (134-130 HU). Pathology from robotic-assisted partial nephrectomy revealed a diagnosis of renal oncocytoma. **Panel B:** Contrast-enhanced CT scan of a 64-year-old male with a right renal mass in the nephrographic phase. An Aorta-Lesion-Attenuation Difference of 44 (144-100 HU) was calculated by placing the largest possible region of interest in the abdominal aorta and renal lesion on the same image slice. Pathology after surgical excision demonstrated a clear cell renal cell carcinoma.

Table 1. Patient demographics and tumor characteristics

		Tumor Histology					
	All N = 227	Angiomyolipoma N = 9 (4%)	Oncocytoma N = 22 (10%)	Chromophobe RCC N = 11 (5%)	Papillary RCC N = 37 (16%)	Clear Cell RCC N = 148 (65%)	*P* Value*
Age, mean (SD) y	59 (12)	53 (10)	67 (11)	63 (15)	59 (11)	58 (11)	.008
Male, n (%)	149 (66)	1 (11)	15 (68)	8 (73)	27 (73)	98 (66)	.011
BMI, mean (SD)	31 (6)	28 (5)	28 (6)	29 (6)	30 (6)	28 (6)	.106
Nephrometry score, n (%)							
4	17 (8)	3 (33)	0 (0)	0 (0)	6 (18)	8 (7)	.153
5	41 (19)	2 (22)	4 (19)	3 (27)	6 (18)	26 (18)	
6	34 (16)	4 (45)	1 (5)	3 (27)	8 (23)	18 (13)	
7	40 (18)	0 (0)	7 (33)	2 (18)	3 (9)	28 (20)	
8	28 (13)	0 (0)	3 (14)	0 (0)	4 (12)	21 (15)	
9	46 (21)	0 (0)	4 (19)	3 (27)	6 (18)	33 (23)	
10	9 (4)	0 (0)	2 (10)	0 (0)	1 (3)	6 (4)	
11	1 (0.5)	0 (0)	0 (0)	0 (0)	0 (0)	1 (1)	
Nephrometry score, median (IQR)	7 (5-9)	5 (4-6)	7 (7-9)	6 (5-9)	6 (5-8)	7 (6-9)	.005
Tumor size, median (IQR)	2.7 (2.0-3.6)	1.4 (0.9-1.8)	3.2 (2.3-3.8)	2.0 (1.5-3.5)	2.8 (2.0-4.0)	2.8 (2.0-3.7)	<.001
Pathologic stage, n (%)							
T1a	152 (79)			8 (73)	28 (76)	116 (80)	.017
T1b	30 (16)			0 (0)	5 (14)	25 (17)	
T2a	3 (2)			1 (9)	1 (2)	1 (1)	
T3a	8 (4)			2 (18)	3 (8)	3 (2)	

Abbreviations: IQR = interquartile range
* Demographics and clinical characteristics were examined using one-way analysis of variance and Kruskal-Wallis tests for normally and non-normally distributed continuous variables, respectively, and chi-square or Fisher's exact tests for categorical variables.

Table 2. Diagnostic performance of ALAD in differentiating malignant and benign renal tumors

	ALAD Threshold	Sensitivity (95% CI)	Specificity (95% CI)	Negative Predictive Value (95% CI)	Positive Predictive Value (95% CI)
Excretory ALAD					
Chromophobe RCC vs oncocytoma	>23	75% (34.9-96.8)	95% (74.0-99.9)	90% (73.0-96.8)	86% (46.1-97.7)
Papillary RCC vs oncocytoma	>23	82% (61.9-93.7)	95% (74.0-99.9)	78% (61.8-88.9)	96% (76.4-99.3)
Clear Cell RCC vs oncocytoma	>17	54% (43.7-64.2)	79% (54.4-93.9)	25% (19.5-31.4)	93% (84.5-97.0)
RCC any vs oncocytoma/AML	>17	63% (54.4-71.4)	70% (48.9-87.4)	26% (19.8-32.8)	92% (86.4-95.8)
RCC any vs oncocytoma	>23	48% (39.1-56.6)	95% (74.0-99.9)	21% (17.5-23.8)	90% (90.4-99.8)
Nephrographic ALAD					
Chromophobe RCC vs oncocytoma	>24	100% (29.2-100)	86% (42.1-99.6)	100%	75% (32.8-94.8)
Papillary RCC vs oncocytoma	>35	94% (72.7-99.9)	100% (59.0-100.0)	88% (51.0-97.9)	100%
Clear Cell RCC vs oncocytoma	>24	77% (63.8-87.7)	86% (42.1-99.6)	33% (21.8-47.2)	98% (86.9-99.6)
RCC any vs oncocytoma/AML	>24	84% (73.4-91.3)	55% (23.4-83.3)	33% (19.1-51.4)	93% (86.6-96.0)
RCC any vs oncocytoma	>24	84% (73.7-91.4)	86% (42.1-99.6)	33% (21.5-47.7)	98% (91.1-99.7)

ALAD, Aorta-Lesion-Attenuation Difference; AML, angiomyolipomas; RCC, renal cell carcinoma.
ALAD threshold was determined by Youden's J statistic and was noted as the best cut-off to differentiate between tumor histology.

histology based on ROC analysis is summarized in Supplemental Table 2 and Supplemental Fig. 1.

The AUC for excretory ALAD to differentiate chRCC from oncocytoma was 0.81 (95% CI: 0.59-1.00). At a threshold value of 23 Hounsfield units (HU) for the excretory ALAD to differentiate chRCC from oncocytoma, the sensitivity, specificity, PPV, and NPV were 75%, 95%, 86%, and 90%, respectively. The AUC for excretory ALAD to differentiate any RCC subtype from benign pathology (oncocytoma and AML) was 0.67 (95% CI: 0.55-0.80). At a threshold value of 17 HU for the excretory ALAD to differentiate any RCC subtype from benign pathology (oncocytoma and AML), the sensitivity, specificity, PPV, and NPV were 63%, 70%, 92%, and 26%, respectively.

Mean ALAD values in the nephrographic phase were 76 ± 16 for AMLs, 63 ± 25 for chRCC, 44 ± 27 for ccRCC, 18 ± 11 for oncocytoma, and 70 ± 27 for papillary RCC (P <.0001, Fig. 2, panel B). The sensitivity, specificity, PPV, and NPV of ALAD in the nephrographic phase to differentiate tumor histology is demonstrated in Table 2. The ability of ALAD in the nephrographic phase to discriminate between renal tumor histology based on ROC analysis is summarized in Supplemental Table 2 and Supplemental Fig. 2.

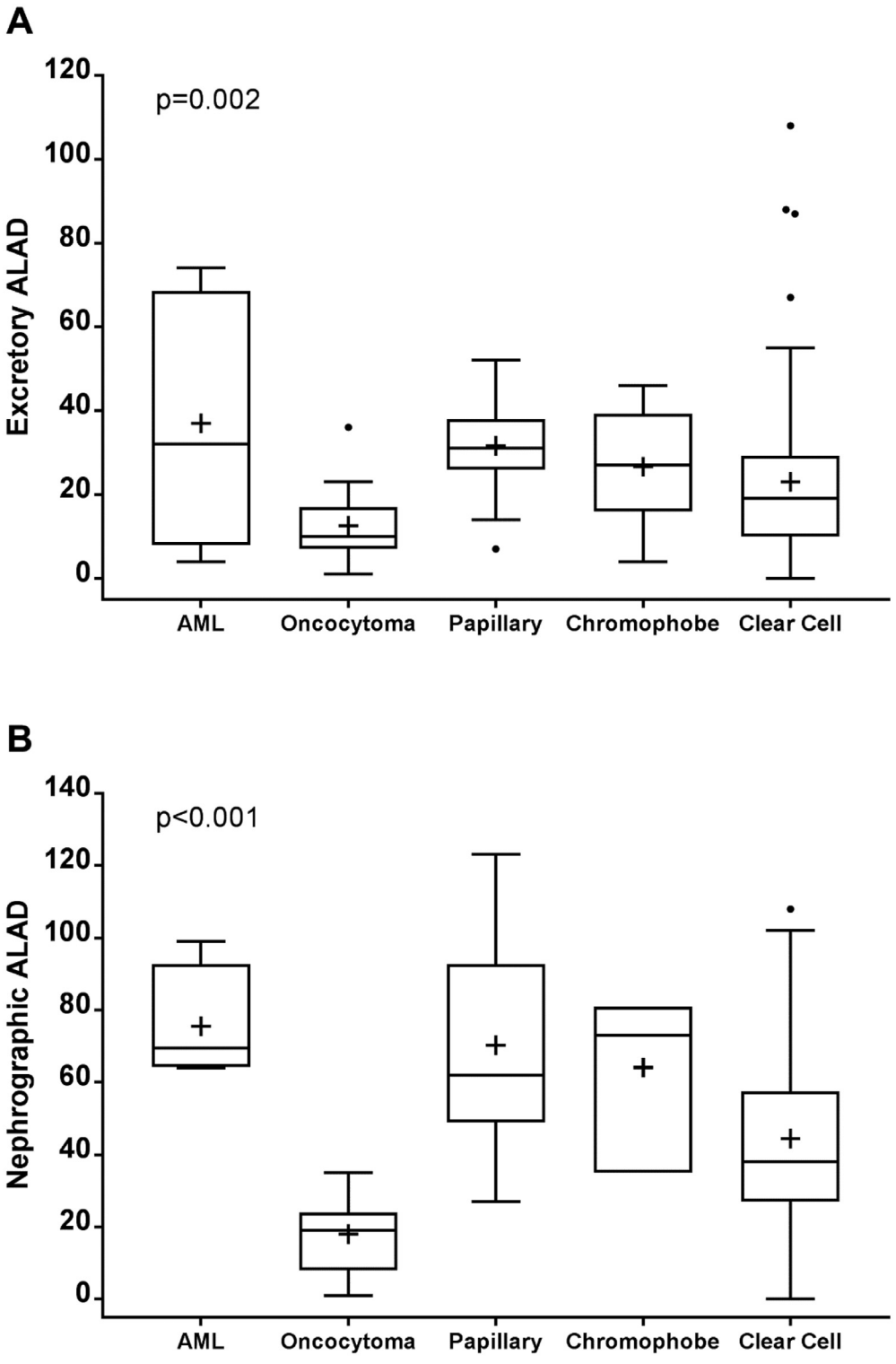

Figure 2. **Panel A:** Distribution of excretory ALAD scores by renal tumor histology. **Panel B:** Distribution of nephrographic ALAD scores by renal tumor histology.

The AUC for nephrographic ALAD to differentiate chRCC from oncocytoma was 0.98 (95% CI: 0.91-1.00). At a threshold value of 24 HU for the nephrographic ALAD to differentiate chRCC from oncocytoma, the sensitivity, specificity, PPV, and NPV were 100%, 86%, 75%, and 100%, respectively. The AUC for nephrographic ALAD to differentiate any RCC subtype from benign pathology (oncocytoma and AML) was 0.63 (95% CI: 0.42-0.84). At a threshold value of 24 HU for the nephrographic ALAD to differentiate any RCC subtype from benign pathology (oncocytoma and AML), the sensitivity, specificity, PPV, and NPV were 84%, 55%, 93%, and 33%, respectively.

DISCUSSION

Pretreatment characterization of SRM remains a clinical challenge with ongoing concerns of overtreatment as well as potential mismatch of treatment modalities to individual patients and their unique renal tumors. Although numerous treatment modalities exist, both surgical and ablative, a significant number of SRM remain indolent, supporting the concept of conservative management with surveillance imaging. These facts, in concert with the significant inroads made in our understanding of unique tumor genomics and biology of RCC subtypes, raise the question of how urologists and radiologists can better characterize SRM (ie, malignant vs benign; high-grade vs low-grade) in the pretreatment setting.

Renal mass biopsy has not historically seen widespread use because of variable data on accuracy, limited utility, and the potential for adverse events.[15] Modern core biopsy techniques demonstrate improved diagnostic accuracy and are generally well-tolerated. Subset pooled analysis of biopsy referenced against surgical pathology in contemporary series revealed sensitivity of 96.3%, specificity of 96.0%, PPV 99.6%, and NPV of 72.7%. Despite high-diagnostic accuracy, 14.1% of biopsies remained non-diagnostic, and the majority of these were determined to be malignant on final surgical pathology.[15] Additionally, it is particularly challenging for pathologists to differentiate oncocytomas from chRCC. Other shortcomings exist regarding biopsy, as not all tumors can be safely biopsied because of anatomic considerations or patient considerations.[16]

There has been recent interest in exploring the use of various noninvasive imaging modalities to provide other means of differentiating benign from malignant renal tumors. The RENAL Nephrometry Score was introduced to standardize renal mass complexity based on tumor size, depth, and location. Further evaluation suggested that the RENAL score might also serve as a predictor of malignant and high-grade pathology.[17] This supported the role of specific imaging characteristics as predictors of tumor behavior and histology. With recent advances in prostate cancer imaging, multiparametric MRI has also been investigated as an imaging tool in evaluating renal tumors. Canvasser et al demonstrated the utility of a multiparametric MRI-based Clear Cell Likelihood Score (ccLS) for the diagnosis of ccRCC histology for cT1a renal masses.[18] Their proposed system demonstrated high specificity and PPV for ccRCC in ccLS 4-5 lesions and high specificity and PPV for non-ccRCC in ccLS 1-2 lesions. Despite good performance in identifying ccRCC, a 10.1% false-positive rate was noted in high−likelihood-RCC lesions, most commonly due to oncocytoma on histology.[18] Cornelius et al demonstrated promising ability of mpMRI to differentiate between various subtypes of RCC compared to standard MRI sequences, but experienced similar challenges on MRI with 94% specificity, but only 19% sensitivity to distinguish ccRCC from oncocytomas.[19] Rosenkrantz et al found no MRI features to reliably differentiate between oncocytoma and chRCC.[20]

Additional promise exists in the field of molecular imaging, which utilizes targeted probes for the detection and characterization of cellular processes.[21,22] Currently utilized in cardiac and parathyroid imaging, 99mTc-sestamibi is a lipophilic cation that accumulates in cells with a high density of mitochondria.[16,22] Oncocytomas are known to have densely packed mitochondria, which initially prompted Gormley et al to pursue this imaging modality to diagnose these tumors over 20 years ago.[21,23] Prospective preoperative imaging with 99mTc-sestamibi SPECT/CT performed in 50 patients with solid clinical T1 renal masses prior to surgical resection correctly identified 5 of 6 (83.3% oncocytomas) and 2 of 2 (100%) hybrid oncocytic/chromophobe tumors, resulting in an overall sensitivity of 87.5% and specificity of 95.2%.[21]

A subsequent pilot study from Sweden again reported a high true positive rate. Upon review of histopathology, 11 of 12 oncocytomas were visually positive on sestamibi imaging, as well as 3 of 3 hybrid oncocytic/chromophobe tumors. Their group again demonstrated that solid lesions without uptake on 99mTc-sestamibi SPECT/CT are most likely malignant and should be surgically resected, while lesions positive on 99mTc-sestamibi are likely benign. Despite these promising results, they concluded that the low-risk of false positive results was non-negligible, with the need to further strengthen 99mTc-sestamibi SPECT/CT potentially by augmenting with standardized, quantitative scoring prior to application in clinical practice.[24]

Dhyani et al introduced ALAD as a novel method to address the conundrum of differentiating benign and malignant oncocytic renal neoplasms found on diagnostic needle biopsy.[10] Their initial evaluation included only oncocytomas and chRCC. Nephrographic-phase ALAD calculations were highly accurate in differentiating chRCC from oncocytoma in the initial (biopsy) dataset (Area under the receiver operating characteristic curve (AUROC) 1.00, 95% CI 1.00-1.00) and the validation (surgical) dataset (AUROC 0.93, 95% CI 0.84-1.00). A threshold value of 25.5 HU demonstrated 100% sensitivity in differentiating chRCC from oncocytoma.[10]

Our current study investigated excretory and nephrographic ALAD performance characteristics in all histologic

subtypes of benign and malignant renal lesions, expanding upon the chRCC and oncocytoma cohorts previously described.[10] Based on AUC analysis, nephrographic ALAD performed better than excretory ALAD in differentiating renal tumor histology with the exception of RCC of any subtype vs benign histology. The discriminative ability of nephrographic ALAD was good or excellent in all comparisons except RCC of any subtype vs benign histology. For example, nephrographic ALAD also provided excellent discrimination in papillary RCC vs oncocytoma (AUC 0.99, 95% CI 0.97-1.00). An ALAD threshold of >35 was 94% sensitive and 100% specific for papillary RCC vs oncocytoma, with 100% PPV. An ALAD threshold of >24 was 100% sensitive and 86% specific for chRCC vs oncocytoma, with 100% NPV. This is the focal point of the current diagnostic conundrum, as no imaging parameter described to date has reliably discriminated between these clinical entities. As a clinical application, preoperative CT scan of an enhancing renal mass with nephrographic ALAD >24 is 93% predictive in discriminating RCC from oncocytoma or AML (the 2 most common benign renal tumors). Additionally, a nephrographic ALAD threshold of >24 identifies all chRCC, and <24 was 100% predictive of oncocytoma. This differentiation has the ability to markedly change treatment and potentially reduce surgical overtreatment.

Our study has several limitations, including the retrospective nature performed at a single tertiary-care institution. Several patients undergoing surgical treatment were excluded due to lack of appropriate imaging, as nephrographic ALAD values could only be calculated in 85 of 227 reviewed patients (37%). This observation warrants further investigation into optimization of preoperative CT scans to more reliably achieve renal enhancement in the nephrographic phase. Patients referred for renal mass evaluation with inability to tolerate an iodinated-contrast CT due to allergy or renal insufficiency were excluded, as were patients who underwent MRI-only or contrasted CT without appropriate nephrographic or excretory phase. Additionally, this represents a single-surgeon series in patients suitable for robotic partial nephrectomy, largely for cT1a renal masses (81%). Patients who opted for active surveillance or thermal ablation were not included in this study, as patients were not deemed to be surgical candidates. To address these limitations, expansion of this series to include multiple surgeons performing radical nephrectomy or partial nephrectomy for cT1 renal masses at our institution is ongoing. Ultimately, prospective multicenter studies should be performed for further validation prior to consideration of widespread incorporation into clinical practice.

CONCLUSION

ALAD measurements based upon preoperative CT scans provide good discrimination between oncocytomas and malignant renal tumors, potentially decreasing the need for diagnostic needle biopsy or treatment in certain patients. ALAD also discriminates well between chRCC and oncocytoma, which may aid in the management of patients with indeterminate diagnoses of oncocytic neoplasm on biopsy. Further validation of ALAD will be necessary prior to routine use in clinical practice.

SUPPLEMENTARY MATERIALS

Supplementary material associated with this article can be found, in the online version, at https://doi.org/10.1016/j.urology.2018.11.036.

References

1. Delahunt B, Srigley JR, Montironi R, Egevad L. Advances in renal neoplasia: recommendations from the 2012 International Society of Urological Pathology Consensus Conference. *Urology*. 2014;83:969–974.
2. Linehan WM, Pinto PA, Bratslavsky G, et al. Hereditary kidney cancer: unique opportunity for disease-based therapy. *Cancer*. 2009;115:2252–2261.
3. Hollingsworth JM, Miller DC, Daignault S, Hollenbeck BK. Rising incidence of small renal masses: a need to reassess treatment effect. *J Natl Cancer Inst*. 2006;98:1331–1334.
4. Lane BR, Babineau D, Kattan MW, et al. A preoperative prognostic nomogram for solid enhancing renal tumors 7 cm or less amenable to partial nephrectomy. *J Urol*. 2007;178:429–434.
5. Frank I, Blute ML, Cheville JC, Lohse CM, Weaver AL, Zincke H. Solid renal tumors: an analysis of pathological features related to tumor size. *J Urol*. 2003;170:2217–2220.
6. Patel HD, Druskin SC, Rowe SP, Pierorazio PM, Gorin MA, Allaf ME. Surgical histopathology for suspected oncocytoma on renal mass biopsy: a systematic review and meta-analysis. *BJU Int*. 2017;119:661–666.
7. Jewett MA, Mattar K, Basiuk J, et al. Active surveillance of small renal masses: progression patterns of early stage kidney cancer. *Eur Urol*. 2011;60:39–44.
8. Gordetsky J, Eich ML, Garapati M, Del Carmen Rodriguez Pena MM, Rais-Bahrami S. Active surveillance of small renal masses. Urology 2018 (in press).
9. Campbell S, Uzzo RG, Allaf ME, et al. Renal mass and localized renal cancer: AUA guideline. *J Urol*. 2017;198:520–529.
10. Dhyani M, Grajo JR, Rodriguez D, et al. Aorta-Lesion-Attenuation-Difference (ALAD) on contrast-enhanced CT: a potential imaging biomarker for differentiating malignant from benign oncocytic neoplasms. *Abdom Radiol*. 2017;42:1734–1743.
11. Gaudiano C, Schiavina R, Vagnoni V, et al. Can the multiphasic computed tomography be useful in the clinical management of small renal masses? *Acta Radiol*. 2017;58:625–633.
12. Choi JH, Kim JW, Lee JY, et al. Comparison of computed tomography findings between renal oncocytomas and chromophobe renal cell carcinomas. *Korean J Urol*. 2015;56:695–702.
13. Pierorazio PM, Hyams ES, Tsai S, et al. Multiphasic enhancement patterns of small renal masses (≤4 cm) on preoperative computed tomography: utility for distinguishing subtypes of renal cell carcinoma, angiomyolipoma, and oncocytoma. *Urology*. 2013;81:1265–1271.
14. Youden WJ. Index for rating diagnostic tests. *Cancer*. 1950;3:32–35.
15. Patel HD, Johnson MH, Pierorazio PM, et al. Diagnostic accuracy and risks of biopsy in the diagnosis of a renal mass suspicious for localized renal cell carcinoma: systematic review of the literature. *J Urol*. 2016;195:1340–1347.
16. Gorin MA, Rowe SP, Allaf ME. Noninvasive determination of renal tumor histology utilizing molecular imaging. *Urol Oncol*. 2016;34:525–528.
17. Kutikov A, Smaldone MC, Egleston BL, et al. Anatomic features of enhancing renal masses predict malignant and high-grade pathology: a preoperative nomogram using the RENAL Nephrometry score. *Eur Urol*. 2011;60:241–248.

18. Canvasser NE, Kay FU, Xi Y, et al. Diagnostic accuracy of multiparametric magnetic resonance imaging to identify clear cell renal cell carcinoma in cT1a renal masses. *J Urol*. 2017;198:780–786.
19. Cornelis F, Tricaud E, Lasserre AS, et al. Routinely performed multiparametric magnetic resonance imaging helps to differentiate common subtypes of renal tumours. *Eur Radiol*. 2014;24:1068–1080.
20. Rosenkrantz AB, Hindman N, Fitzgerald EF, Niver BE, Melamed J, Babb JS. MRI features of renal oncocytoma and chromophobe renal cell carcinoma. *AJR Am J Roentgenol*. 2010;195:W421–W427.
21. Gorin MA, Rowe SP, Baras AS, et al. Prospective evaluation of (99m)Tc-sestamibi SPECT/CT for the diagnosis of renal oncocytomas and hybrid oncocytic/chromophobe tumors. *Eur Urol*. 2016;69:413–416.
22. Rowe SP, Gorin MA, Gordetsky J, et al. Initial experience using 99mTc-MIBI SPECT/CT for the differentiation of oncocytoma from renal cell carcinoma. *Clin Nucl Med*. 2015;40:309–313.
23. Gormley TS, Van Every MJ, Moreno AJ. Renal oncocytoma: preoperative diagnosis using technetium 99m sestamibi imaging. *Urology*. 1996;48:33–39.
24. Tzortzakakis A, Gustafsson O, Karlsson M, Ekström-Ehn L, Ghaffarpour R, Axelsson R. Visual evaluation and differentiation of renal oncocytomas from renal cell carcinomas by means of. *EJNMMI Res*. 2017;7:29.